# Comparison of the Efficiency of Complexes Based on S4₁₃-PV Cell-Penetrating Peptides in Plasmid DNA and siRNA Delivery

Ana M. Cardoso,[†] Sara Trabulo,[†,∥] Ana L. Cardoso,[†] Sílvia Maia,[‡] Paula Gomes,[‡] Amália S. Jurado,[†,§] and Maria C. Pedroso de Lima*[,†,§]
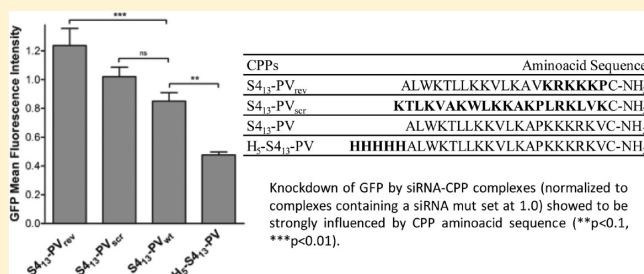
[†]CNC - Centre for Neuroscience and Cell Biology, University of Coimbra, Portugal
[‡]CIQUP, Department of Chemistry and Biochemistry, University of Porto, Portugal
[§]Department of Life Sciences, University of Coimbra, Portugal

**ABSTRACT:** The successful application of gene therapy approaches is highly dependent on the efficient delivery of nucleic acids into target cells. In the present study, new peptide-based nonviral systems were developed to enhance plasmid DNA and siRNA delivery, aiming at generating appropriate gene delivery and gene silencing tools for preclinical and clinical application. For this purpose, a new cell-penetrating peptide derived from the wild-type S4₁₃-PV peptide was synthesized through the addition of a five-histidine tail to its *N*-terminus (H₅-S4₁₃-PV), and its ability to mediate gene expression and gene silencing was evaluated and compared to that of the wild-type peptide. The histidine-enriched peptide, H₅-S4₁₃-PV, proved to be generally more efficient and less toxic than the wild-type peptide in the delivery of plasmid DNA. In addition, complexes of H₅-S4₁₃-PV with siRNAs, but not of S4₁₃-PV, were efficiently internalized by cells and presented high knockdown activity (63%). Interestingly, systems containing the S4₁₃-PV or the H₅-S4₁₃-PV peptide exhibited superior biological activity when compared to those containing the reverse NLS or scrambled peptides, suggesting that both the cell-penetrating sequence and the NLS of the S4₁₃-PV peptide influence the competence of binary and ternary complexes to accomplish nucleic acid delivery. In order to unravel the cancer therapeutic potential of formulations with the histidine-enriched peptide, their efficiency to mediate silencing of the oncogenic protein survivin was evaluated. As opposed to complexes with the wild-type peptide, H₅-S4₁₃-PV complexes showed the ability to promote a high survivin knockdown at the level of both protein (44%) and mRNA (73%), in HT1080 cells.

**KEYWORDS:** *cell-penetrating peptide, cationic liposome, cancer gene therapy, survivin, RNA interference*

| CPPs | Aminoacid Sequence |
|---|---|
| S4₁₃-PV$_{rev}$ | ALWKTLLKKVLKAV**KRKKKP**C-NH₂ |
| S4₁₃-PV$_{scr}$ | **KTLKVAKWLKKAKPLRKLV**KC-NH₂ |
| S4₁₃-PV | ALWKTLLKKVLKAPKKKRKVC-NH₂ |
| H₅-S4₁₃-PV | **HHHHH**ALWKTLLKKVLKAPKKKRKVC-NH₂ |

Knockdown of GFP by siRNA-CPP complexes (normalized to complexes containing a siRNA mut set at 1.0) showed to be strongly influenced by CPP aminoacid sequence (**p<0.1, ***p<0.01).

## INTRODUCTION

In order to improve the clinical efficacy of gene-based therapeutic strategies, a great deal of effort has been expended on the discovery of potent therapeutic genes or gene-modulating molecules and on the enhancement of the efficiency of gene delivery systems. Viral and nonviral systems have been developed to mediate the delivery of plasmid DNA and siRNAs to target cells. However, gene therapy approaches that are both highly efficient and clinically viable are still scarce.[1−3] Cell-penetrating peptides (CPPs) have been extensively applied for nucleic acid delivery, using both covalent and noncovalent association strategies.[4] While the covalent linkage of CPPs to nucleic acids allows the formation of small, monomeric conjugates of known stoichiometry with high reproducibility, the preparation of noncovalent complexes is technically simpler, originates nanoparticles with a net positive charge, and decreases the risk of altering the biological activity of the cargo.[4,5]

Many CPPs are derived from transduction domains of proteins, which are known for their remarkable properties of cell penetration, although model and designed CPPs have also

been generated. Several modifications of naturally occurring sequences have been introduced in CPPs in order to achieve higher transfection efficiencies mediated by CPP-based delivery systems. A new HIV-1 Tat peptide-based gene delivery system was designed by fusing the original Tat with cysteine and histidine residues.[6] The rationale behind these modifications was based on the features of these amino acids. The cysteine residue−disulfide interactions allow the stabilization and protection of the CPP−nucleic acid complexes in the extracellular medium, while their lability in the endosomal reducing environment contributes to nucleic acid release. However, the specific p$K_a$ of the histidine imidazole group, being close to the endosomal pH, allows protonation and leads to osmotic swelling, mimicking the proton−sponge effect observed with polyethyleneimine (PEI), thus facilitating nucleic acid release.[6−8] Proton−sponge activity has been exploited in

the CPP field by using peptides that partially mimic this feature. With this purpose, lysine and histidine residues have been added to template amphipathic peptides rich in alanines and leucines.[9] Lysines were expected to promote DNA condensation, conferring positive charge to the peptides, while histidines might favor the endosomal escape of DNA by the above-mentioned process.[8] Various numbers of lysine and histidine residues were included in the original peptide sequence, either by replacement of a neutral amino acid or by the addition of a new residue to the sequence. The transfection efficiency showed the dependence on the number of histidine residues and on their position in the sequence, as well as on the pH at which the peptides change from an in-plane to a trans-membrane alignment, the most efficient peptides being those containing 4 to 5 histidines located in the polar face of the $\alpha-$ helix structure.[9] On the basis of all these findings, modifications were performed on the $S4_{13}$-PV peptide, a dermaseptin derived peptide fused to the nuclear localization sequence of the SV40 large T antigen,[10] which has been extensively studied in our laboratory. In this regard, a $S4_{13}$-PV analogue with a five-histidine tail at the N-terminus was synthesized, originating a new peptide called herein $H_5$-$S4_{13}$-PV. Following our previous work on the development of $S4_{13}$-PV peptide-based vectors for nucleic acid delivery[9,10] and aiming at identifying the molecular features responsible for efficient nucleic acid delivery, the new peptide was here compared with the wild-type ($S4_{13}$-PV) and its scrambled ($S4_{13}$-PV$_{scr}$) and reverse NLS ($S4_{13}$-PV$_{rev}$) analogues (Table 1), in terms of its ability to efficiently deliver

**Table 1. Sequences of the $S4_{13}$-PV and Derived Peptides Used in the Present Study**

| | |
|---|---|
| $S4_{13}$-PV | ALWKTLLKKVLKAPKKKRKVC-NH$_2$ |
| $H_5$-$S4_{13}$-PV | HHHHHALWKTLLKKVLKAPKKKRKVC-NH$_2$ |
| $S4_{13}$-PV$_{scr}$ | KTLKVAKWLKKAKPLRKLVKC-NH$_2$ |
| $S4_{13}$-PV$_{rev}$ | ALWKTLLKKVLKAVKRKKKKPC-NH$_2$ |

plasmid DNA and siRNA to different cell lines. Ternary systems produced through the addition of dioleoyltrimethyl-lammoniumpropane: dioleoylphosphatidylethanolamine (DO-TAP:DOPE) liposomes to the CPP-nucleic acid complexes were also assayed since previous work had revealed that the association of these vesicles with CPP complexes led to the formation of more efficient plasmid delivery systems.[11,12]

Our results showed that the histidine tail preserves or improves the $S4_{13}$-PV peptide's ability to efficiently deliver reporter plasmid DNA and siRNAs to different cell lines. In order to test the efficiency of the new CPP-based delivery systems to silence endogenous genes, the survivin gene was selected as a target. Survivin is a member of the IAP family, playing an important role in cell proliferation and inhibition of apoptosis.[13−22] Because of its overexpression in cancer cells and no or very low expression in normal cells, survivin constitutes a particularly promising target for cancer therapy. Moreover, survivin renders malignant cells resistant to conventional antitumoral treatments, by counteracting pro-apoptotic stimuli and, therefore, enhancing cancer cell survival.[11,21−25]

Altogether, the present findings open a new window to extend the use of CPPs, including the $S4_{13}$-PV peptide and its histidine derivative, as appropriate tools for nucleic acid delivery, with potential for clinical applications in different pathologies, such as cancer.

## ■ MATERIALS AND METHODS

**Materials.** The cationic lipid 1,2-dioleoyl-3-trimethylammo-nium-propane (DOTAP) and 1,2-dioleoyl-sn-glycero-3-phos-phoethanolamine (DOPE) were purchased from Avanti Polar Lipids (Alabaster, AL, USA). The primers for survivin and for HPRT-1 genes were predesigned by Qiagen (QuantiTect Primer, Qiagen). The antibody antisurvivin was purchased from Santa Cruz (Santa Cruz Biotechnology, Inc., Heidelberg, Germany), and the remaining antibodies were obtained from Sigma (St. Louis, MO, USA). The anti-GFP siRNA (5′-GCAAGCUGACCCUGAAGUUCAU-3′) and Cy3-labeled nonspecific siRNA sequence were purchased from Ambion (Austin, TX, USA). The antisurvivin siRNA (5′-GGACCA-CCGCAUCUCUACAdTdT-3′) and the nonsilencing siRNA used as control were obtained from Dharmacon (Lafayette, CO, USA). Fmoc-protected amino acids, Fmoc-Rink amide-MBHA LL resin (0.36 mmol/g) and coupling reagent O-(benzotriazol-1-yl)-N,N,N′,N′-tetramethyluronium-hexafluoro-phosphate (HBTU) were provided by Novabiochem (VWR International, Portugal). All the other chemicals were of the highest grade.

**Peptide Synthesis.** Peptide synthesis was performed using a Liberty Microwave Peptide Synthesizer (CEM Corporation, Mathews, NC, USA). Peptide analysis by HPLC was done using a Hitachi-Merck LaChrom Elite system equipped with a quaternary pump, a thermostatted (Peltier effect) automated sampler, and a diode-array detector (DAD). An LCQ-DecaXP LC-MS system from ThermoFinnigan, equipped with both a DAD detector and an electrospray ionization-ion trap mass spectrometer (ESI/IT MS), was also used for peptide analysis. Peptide quantitation was performed by measuring the absorbance at 280 nm in a Helios Gama spectrophotometer (Spectronic Unicam).

The peptide (C-terminal amide) was assembled by Fmoc/tBu solid-phase peptide synthesis (SPPS) methodologies assisted with microwave (MW) energy.[26] The resin was preconditioned for 15 min in N,N-dimethylformamide (DMF) and then transferred into the MW-reaction vessel. The initial Fmoc deprotection step was carried out using 20% piperidine in DMF containing 0.1 M of 1-hydroxybenzotriazole (HOBt) in two MW irradiation pulses: 30 s at 24 W plus 3 min at 28 W, in both cases temperature being no higher than 75 °C. The C-terminal amino acid was then coupled to the deprotected Rink amide resin, using 5 mol equivalent (eq) of the Fmoc-protected amino acid in DMF (0.2 M), 5 eq of 0.5 M HBTU/HOBt in DMF, and 10 eq of 2 M N-ethyl-N,N-diisopropylamine (DIPEA) in N-methylpyrrolidone (NMP); the coupling step was carried out for 5 min at 35 W MW irradiation, with maximum temperature reaching 75 °C. The remaining amino acids were sequentially coupled in the C→N direction by means of similar deprotection and coupling cycles, except for the incorporation of (i) Fmoc-Arg(Pbf)-OH, whose coupling was done in two steps, 25 min with no MW irradiation (room temperature) followed by 5 min coupling at 25 W; (ii) Fmoc-Cys(Trt)-OH, Fmoc-Trp(Boc)-OH, and Fmoc-His-(Trt)-OH, all coupled also in two steps, first with 2 min coupling without MW irradiation (room temperature), then followed by 4 min coupling at 25 W, with maximum temperature reaching 50 °C. Double-coupling was employed with all lysines in the sequence (residues 5, 6, 7, 10, and 14), incorporated as Fmoc-Lys(Boc)-OH. Following completion of the sequence assembly, the peptide was released from the resin

with concomitant removal of side-chain protecting groups, by a 3 h acidolysis at room temperature using a trifluoroacetic acid (TFA)-based cocktail[27,28] containing thioanisole, 1,2-ethanedithiol, and anisole as scavengers (TFA/thioanisole/1,2-ethanedithiol/anisole 90:5:3:2 v/v/v/v). Crude product was purified by reverse-phase liquid chromatography to give the target peptide, as confirmed by HPLC, LC-ESI/IT MS, and AAA.

**Cells.** HeLa cells (human epithelial cervical carcinoma) and A549 cells (human epithelial lung adenocarcinoma) were maintained at 37 °C, under 5% $CO_2$, in Dulbecco's modified Eagle's medium-high glucose (DMEM; Sigma) supplemented with 10% (v/v) heat-inactivated fetal bovine serum (FBS; Biochrom KG) and 100 units penicillin and 100 $\mu$g of streptomycin (Sigma) per mL. HT1080 cells (human fibrosarcoma) were maintained at 37 °C, under 5% $CO_2$, in Dulbecco's modified Eagle's low glucose medium (DMEM-LG; Sigma) supplemented with 10% (v/v) heat-inactivated fetal bovine serum (FBS; Biochrom KG) and 100 units penicillin and 100 $\mu$g of streptomycin (Sigma) per mL.

For flow cytometry and cell viability experiments, $1.0 \times 10^5$ HeLa, A549, or HT1080 cells/well were seeded onto 12-well plates; for fluorescence microscopy studies, $0.2 \times 10^5$ HT1080 cells/well were plated onto 8-well chambered coverslips (Lab-Tek II Chamber Slide System Nunc). For QRT-PCR and Western blot experiments, $1.0 \times 10^5$ HeLa, A549, and HT1080 cells/well were plated onto 6-well plates. Cells were plated 24 hours prior to incubation with the complexes.

**Cationic Liposome Preparation.** Small unilamellar vesicles (SUV) were prepared by extrusion of multilamellar vesicles composed of the cationic lipid DOTAP and DOPE at a 1:2 molar ratio. Briefly, lipid solutions in chloroform were mixed at the desired molar ratio and dried under vacuum, at room temperature, using a rotary evaporator. The dried lipid films were then hydrated with 1.0 mL of high purity water, and the obtained multilamellar vesicles were briefly sonicated and extruded 21 times through two stacked polycarbonate filters (50 nm pore diameter) using a Liposofast device (Avestin). The lipid concentration of the resulting SUV was determined by the Bartlett method,[29] which measures the inorganic phosphate released after the hydrolysis of dried phospholipids, at 180 °C, in 70% $HClO_4$.[30]

**Complex Preparation.** The complexes (binary and ternary) were prepared in HEPES-buffered saline solution (HBS; 140 mM NaCl and 10 mM HEPES, pH 7.4). Binary complexes were produced by gently mixing the plasmid DNA (0.5 $\mu$g) or the siRNA (25 pmol) with each of the CPPs, at the desired charge ratio, followed by 15 min (plasmid DNA complexes) or 30 min (siRNA complexes) of incubation at room temperature. Ternary plasmid DNA complexes were obtained by gently mixing peptide/pDNA complexes, prepared at the desired charge ratio, with DOTAP:DOPE liposomes. Mixtures were then incubated for 15 min, at room temperature. SiRNA formulations containing both CPP and cationic liposomes were prepared following two different protocols, which involved the addition of each CPP to the siRNAs, followed by the addition of the cationic liposomes (herein termed CPP/siRNA/DOTAP:DOPE complexes), or the mixing of the CPPs with the cationic liposomes, before the addition of the siRNAs (herein termed CPP/DOTAP:DOPE/siRNA complexes). After the addition of each component, the mixtures were gently mixed and incubated for 30 min at room temperature to allow for the formation of the complexes exhibiting the desired charge ratios.

**Physicochemical Characterization of Complexes.** Complexes were characterized with respect to their size by photon correlation spectroscopy-based technique (PCS) using a Coulter N4 Plus (Coulter Corporation, Miami, FL, USA). PCS uses autocorrelation spectroscopy of scattered laser light to determine its time-dependent fluctuations resulting from the Brownian motion of particles in suspension. The light intensity scattered at a given angle is detected by a photomultiplier (at fixed angle of 90°) whose output current is passed to an autocorrelator, which analyses time dependence, determining the rate of diffusion or Brownian motion of the particles and hence their size.[31] Complexes were prepared immediately before analysis. All complexes showed a polymodal size distribution.

Zeta potential measurements of different complexes were performed using a Nano ZS, ZN 3500 (Malvern Instruments, UK). The Nano ZS is a laser-based multiangle particle electrophoresis analyzer that measures the electrophoretic mobility and zeta potential distribution simultaneously with the hydrodynamic size of particles in suspension. CPP/DNA and CPP/DNA/liposomes complexes were prepared immediately before analysis. Samples of the prepared complexes were placed in the DTS 1060C measuring cell, whose position was adjusted to cover a previously determined stationary layer, and an electric current of 3.0 mA was applied.

Measurements were recorded, and the zeta potential was calculated for each scattering angle (8.6°, 17.1°, 25.6°, and 34.2°). Data represent the mean ± SD obtained for the different angles of three measurements. All complexes showed a unimodal distribution for the zeta potential

**Cell Transfection.** Twenty-four hours after plating, cells were incubated with 100 $\mu$L of the complexes (binary and ternary) containing plasmid DNA (1 $\mu$g/mL) or siRNA (50 nM), in a final volume of 500 $\mu$L of antibiotic- and serum-free OptiMEM (Invitrogen, CA, USA), for 4 h at 37 °C. After this incubation period, the transfection medium was replaced with fresh medium containing 10% (v/v) FBS plus antibiotics, and the cells were further incubated for 44 h to allow gene expression/silencing. The efficiency of transfection and knockdown mediated by the different complexes was evaluated by analyzing GFP expression by flow cytometry, as described below.

**Analysis of GFP Expression by Flow Cytometry.** Flow cytometry analysis of GFP expression was performed in live cells using a Becton Dickinson FACSCalibur flow cytometer (BD Biosciences, San Jose, CA, USA). Data were obtained and analyzed using CellQuest software. Forty-eight hours after transfection, the cells (HeLa, A549 or HT1080) were washed once with PBS and detached with trypsin (10 min at 37 °C). The cells were then further washed, resuspended in cold PBS, and immediately analyzed. To discriminate between viable and dead cells and to exclude doublets, cells were appropriately gated by forward/side scatter and pulse width from a total of 10,000 events. The FITC bandpass filter was used in emission detection. GFP expression was evaluated through the analysis of the percentage of transfected cells and of the geometric mean fluorescence intensity with respect to control cells (nontransfected cells). GFP silencing was evaluated through the analysis of the fluorescence intensity with respect to cells treated with siRNA mut (scrambled sequence) complexes.

**Analysis of siRNA Internalization and Intracellular Distribution by Confocal Microscopy.** HT1080 cells ($0.2 \times 10^5$ cells/well) were plated onto 8-well chambered coverslips.

Following overnight culture, the cells were treated for 4 h with the different delivery systems, formulated with Cy3-labeled siRNAs (50 nM), in OptiMEM medium. After this period, or following further 20 h of incubation in serum-containing medium, cells were rinsed twice with PBS and incubated with Hoechst 33342 dye (1 $\mu$g/mL, Molecular Probes, Eugene, OR). Cells were then rinsed twice with PBS and directly observed in the chambers in 0.5 mL of OptiMEM. Fluorescence distribution inside live cells was analyzed under a Zeiss Axiovert 200 M fluorescence microscope (Carl Zeiss, Oberk), using the 60× oil immersion objective.

**Extraction of RNA and cDNA Synthesis.** RNA was recovered from A549, HeLa, and HT1080 cells, 48 h after cell transfection, using the MasterPure RNA Purification Kit (Epicenter Biotechnologies, Madison, WI, USA) according to the manufacturer's instructions, and then treated with DNase I. Briefly, cells were lysed using the Tissue and Cell Lysis Solution from the MasterPure RNA Purification Kit containing proteinase K, and cell lysates were collected to microcentrifuge tubes. MPC Protein Precipitation Reagent was added to the protein extract from the lysates. Then, 500 $\mu$L of isopropanol was added to the recovered supernatant to promote total nucleic acid precipitation, which was pelleted by centrifugation. Removal of contaminating DNA from the RNA was then performed by the addition of a DNase I solution and carrying out another step of protein removal using MPC Protein Precipitation Reagent. RNA was finally pelleted by centrifugation, rinsed twice with 70% ethanol, and resuspended in TE buffer. After quantification, RNA was converted to cDNA using the Superscript III First Strand Synthesis Kit (Invitrogen, Karlsruhe, Germany), according to the manufacturer's instructions.

**Quantitative Real Time Polymerase Chain Reaction (QRT-PCR).** Quantitative PCR was performed in an iQ 5 thermocycler using 96-well microtiter plates and the iQ SYBR Green Supermix Kit, as described before.[32] The primers for the target gene (survivin) and the reference gene (HPRT-1) were predesigned by Qiagen (QuantiTect Primer, Qiagen). Survivin mRNA fold decrease with respect to control samples was determined by the Pfaffl method,[33] taking into consideration the different amplification efficiencies of both genes in all experiments. The amplification efficiency for each target or reference gene was determined according to the equation: $E = 10^{-1/S}-1$, where $S$ is the slope of the obtained standard curve.

**Western Blot Analysis.** Seventy-two hours after transfection of cells (HeLa, A549, or HT1080 cells) with the siRNA complexes, total protein extracts were obtained using a lysis buffer (50 mM NaCl, 50 mM EDTA, and 1% Triton X-100) supplemented with a protease inhibitor cocktail (Sigma), 10 $\mu$g/mL DTT, and 1 mM PMSF. Protein content was determined using the Bio-Rad DC protein assay (Bio-Rad). For each sample, 20 $\mu$g of total protein was resuspended in loading buffer (20% glycerol, 10% SDS, and 0.1% bromophenol blue), incubated for 5 min at 95 °C, and loaded onto a 15% polyacrylamide gel. After electrophoresis, the proteins were blotted onto a PVDF membrane according to standard protocols. After blocking in 5% nonfat milk, the membrane was incubated overnight at 4 °C with the appropriate primary antibody (antisurvivin 1:200, Santa-Cruz) and thereafter with the appropriate secondary antibody (1:10000, Sigma) for 2 h at room temperature. Equal protein loading was shown by reprobing the membrane with an anti-$\alpha$-tubulin antibody (1:10000, Sigma) and with the appropriate secondary antibody.

After this incubation period, the membrane was washed several times with saline buffer (TBS/T containing 25 mM Tris−HCl, 150 mM NaCl, 0.1% Tween, and 5 mg/mL nonfat powder milk), incubated with ECF (alkaline phosphatase substrate; 20 $\mu$L of ECF/cm² of membrane) for 5 min at room temperature, and submitted to fluorescence detection at 570 nm using a VersaDoc Imaging System Model 3000 (Bio-Rad). For each membrane, the analysis of band intensity was performed using Image J software (Wayne Rasband National Institutes of Health, USA), and the survivin band intensities were normalized to $\alpha$-tubulin in each experiment.

**Evaluation of Cell Viability.** Cell viability was assessed under the different experimental conditions by a modified Alamar Blue assay, as described previously.[34] Briefly, 48 h (for flow cytometry and QRT-PCR analysis) or 72 h (for Western blot analysis) after transfection, the cells were incubated with DMEM (HeLa and A549 cells) or DMEM-LG (HT1080 cells) containing 10% (v/v) resazurin dye. After 1 h of incubation at 37 °C, the absorbance of the medium was measured at 570 and 600 nm. Cell viability was calculated as a percentage of control cells (nontransfected cells), according to the following equation:

$$\text{cell viability (\% of control)} = [(A_{570} - A_{600})/(A'_{570} - A'_{600})] \times 100$$

where $A_{570}$ and $A_{600}$ are the absorbances of the samples, and $A'_{570}$ and $A'_{600}$ are the absorbances of control cells, at the indicated wavelengths.

## RESULTS

**Physicochemical Characterization of Complexes.** Because the efficacy to deliver genetic material inside target cells is strongly dependent on the physicochemical properties of the carrier systems, the different complexes used in the present study were characterized with respect to their size and surface charge density. As shown in Table 2, lipoplexes prepared from DOTAP:DOPE (1:2 molar ratio) cationic liposomes at the 1/1 lipid/DNA (+/−) charge ratio exhibited the smallest mean diameter (approximately 240 nm) and the most negative zeta potential (−27.1 mV). Binary complexes prepared with the S4$_{13}$-PV or with the H$_5$-S4$_{13}$-PV peptides at different charge ratios (5/1 and 10/1) exhibited mean diameters of 655 to 1400 nm, along with slightly positive zeta potentials. Addition of DOTAP:DOPE (1:2 molar ratio) cationic liposomes to any of the peptide/DNA complexes resulted in a significant increase in the size of the resulting complexes (approximately 2100−2700 nm), except for the ternary complexes of the histidine derivative formulated at the 10/1/1 ratio, which maintained the same size as their binary counterpart (665 nm). The surface charge values for these complexes were generally positive and close to neutrality.

**Plasmid DNA Delivery Mediated by S4$_{13}$-PV- and H$_5$-S4$_{13}$-PV-Based Vectors.** In order to comparatively evaluate the biological activity of the S4$_{13}$-PV peptide, previously used as a component in plasmid DNA delivery systems,[11] and that of a new histidine-enriched derivative (H$_5$-S4$_{13}$-PV), cell viability and transfection experiments were performed in two tumoral cell lines (HeLa and A549). Complexes of each peptide with a plasmid DNA encoding the GFP gene were prepared, either per se or in combination with DOTAP:DOPE (1:2 molar ratio) liposomes, using the order of component addition that was previously shown to originate complexes with the highest

**Table 2. Mean Diameter and Zeta Potential of the Plasmid DNA Complexes**

| | size (nm)[a] | zeta potential (mV)[a] |
|---|---|---|
| DOTAP:DOPE/pDNA 1/1 | 239.4 (±47.1) | −27.1 (±3.0) |
| S4$_{13}$-PV/pDNA 5/1 | 1412.0 (±485.4) | +9.9 (±4.4) |
| S4$_{13}$-PV/pDNA 10/1 | 1191.3 (±176.7) | +9.6 (±3.8) |
| H$_5$-S4$_{13}$-PV/pDNA 5/1 | 1108.5 (±168.7) | +9.6 (±4.4) |
| H$_5$-S4$_{13}$-PV/pDNA 10/1 | 654.8 (±110.1) | +12.3 (±4.5) |
| S4$_{13}$-PV/pDNA/DOTAP:DOPE 2/1/1 | 2628.6 (±401.9) | +9.2 (±3.8) |
| S4$_{13}$-PV/pDNA/DOTAP:DOPE 5/1/1 | 2157.1 (±836.5) | +0.3 (±5.0) |
| S4$_{13}$-PV/pDNA/DOTAP:DOPE 10/1/1 | 2348.2 (±938.6)** | +7.2 (±3.2) |
| H$_5$-S4$_{13}$-PV/pDNA/DOTAP:DOPE 2/1/1 | 2627.8 (±435.4) | +8.6 (±4.1) |
| H$_5$-S4$_{13}$-PV/pDNA/DOTAP:DOPE 5/1/1 | 2762.7 (±359.1)*** | +13.0 (±3.3) |
| H$_5$-S4$_{13}$-PV/pDNA/DOTAP:DOPE 10/1/1 | 665.1 (±100.4) | −5.6 (±2.8) |

[a]Results represent the mean ± SD from three independent experiments. Data comparisons were performed between formulations containing S4$_{13}$-PV and H$_5$-S4$_{13}$-PV (no significance) and between S4$_{13}$-PV/pDNA or H$_5$-S-S4$_{13}$-PV/pDNA and the corresponding ternary complexes containing DOTAP:DOPE (**$p < 0.01$; ***$p < 0.001$).

transfection ability.[35] The viability of A549 and HeLa cells (Figure 1) was determined following exposure to the peptide-based binary complexes (S4$_{13}$-PV/pDNA or H$_5$-S4$_{13}$-PV/pDNA) and ternary complexes (S4$_{13}$-PV/pDNA/DOTAP:DOPE or H$_5$-S4$_{13}$-PV/pDNA/DOTAP:DOPE), as well as to DOTAP:DOPE/pDNA and lipofectamine/pDNA lipoplexes (used as positive controls). HeLa cells (Figure 1A) were shown to be more susceptible to complex-mediated cytotoxicity than A549 cells (Figure 1B), particularly at the highest peptide/

DNA (+/−) charge ratios. The tested formulations did not significantly affect the viability of A549 cells (Figure 1B), especially when compared to that of the commercially available transfection reagent Lipofectamine 2000. In HeLa cells, the wild-type CPP (S4$_{13}$-PV) was more toxic than its histidine derivative, when formulated both in binary and ternary complexes. This cytotoxic effect was mostly significant for the formulations with high peptide amounts, i.e., CPP/pDNA at a 10/1 charge ratio and CPP/pDNA/DOTAP:DOPE at a 10/1/1 charge ratio. In these cases, the cell viability in the presence of complexes containing the wild-type peptide was about 30% of that observed in the presence of complexes prepared with the new histidine-enriched peptide, although the former complexes were more efficient in transfecting HeLa cells (see Figure 2A) than the corresponding complexes prepared with the H$_5$-S4$_{13}$-PV peptide.

The ability of formulations assayed for cell viability, as described in Materials and Methods, to transfect HeLa and A549 cells was assessed by flow cytometry analysis. Figure 2 presents the percentage of transfected cells (A and C) and the mean GFP fluorescence intensity (B) obtained with CPP-based complexes in both cells lines. Regarding HeLa cells, a highly transfectable cell line, the highest number of transfected cells was achieved with the binary (80.1%) and ternary (77.7%) complexes containing the wild-type CPP, prepared at 10/1 and 10/1/1 (+/−) charge ratios, respectively. Both values were higher than that obtained with Lipofectamine 2000 (74.0% of transfected cells). As observed, the H$_5$-S4$_{13}$-PV peptide, although unable to efficiently deliver plasmid DNA to HeLa cells when formulated in a binary complex (achieving only approximately 11% of transfected cells), was able to transfect a considerable number of cells (approximately 60%) when present in ternary complexes at 5/1/1 and 10/1/1 peptide/pDNA/lipid charge ratios. Regarding the mean fluorescence intensity, which represents the average amount of DNA copies
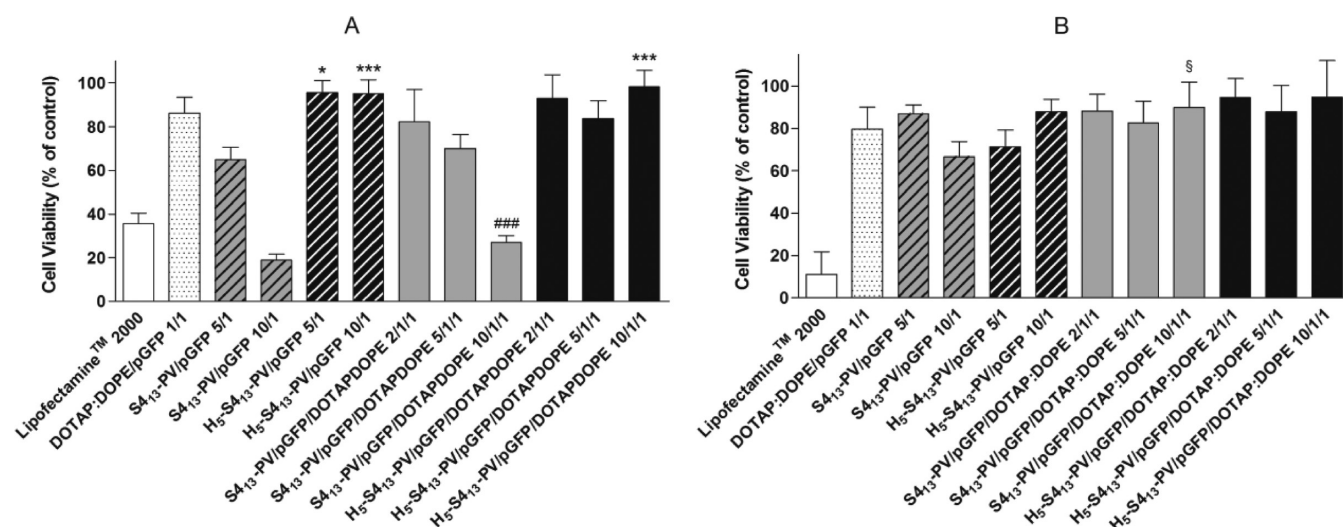


**Figure 1.** Cell viability in the presence of different CPP-based gene delivery systems. HeLa (A) and A549 (B) cells were incubated with the different complexes containing 1 μg/mL of GFP-encoding plasmid DNA for 4 h, following an additional 44 h of incubation with complete medium. After this period, cell viability was determined by a modified Alamar Blue assay as described in Materials and Methods. Complexes of DNA with DOTAP:DOPE and with Lipofectamine 2000 were used for comparison. Cell viability is expressed as a percentage of the control (nontransfected cells). All results are presented as the mean ± SD of at least three independent experiments. Data comparisons were performed between formulations containing S4$_{13}$-PV and H$_5$-S4$_{13}$-PV (*$p < 0.05$; ***$p < 0.001$), between DOTAP:DOPE/pDNA lipoplexes and the same lipoplexes containing S4$_{13}$-PV or H$_5$-S4$_{13}$-PV (###$p < 0.001$) and between S4$_{13}$-PV/pDNA or H$_5$-S4$_{13}$-PV/pDNA and the corresponding ternary complexes containing DOTAP:DOPE (§$p < 0.05$).
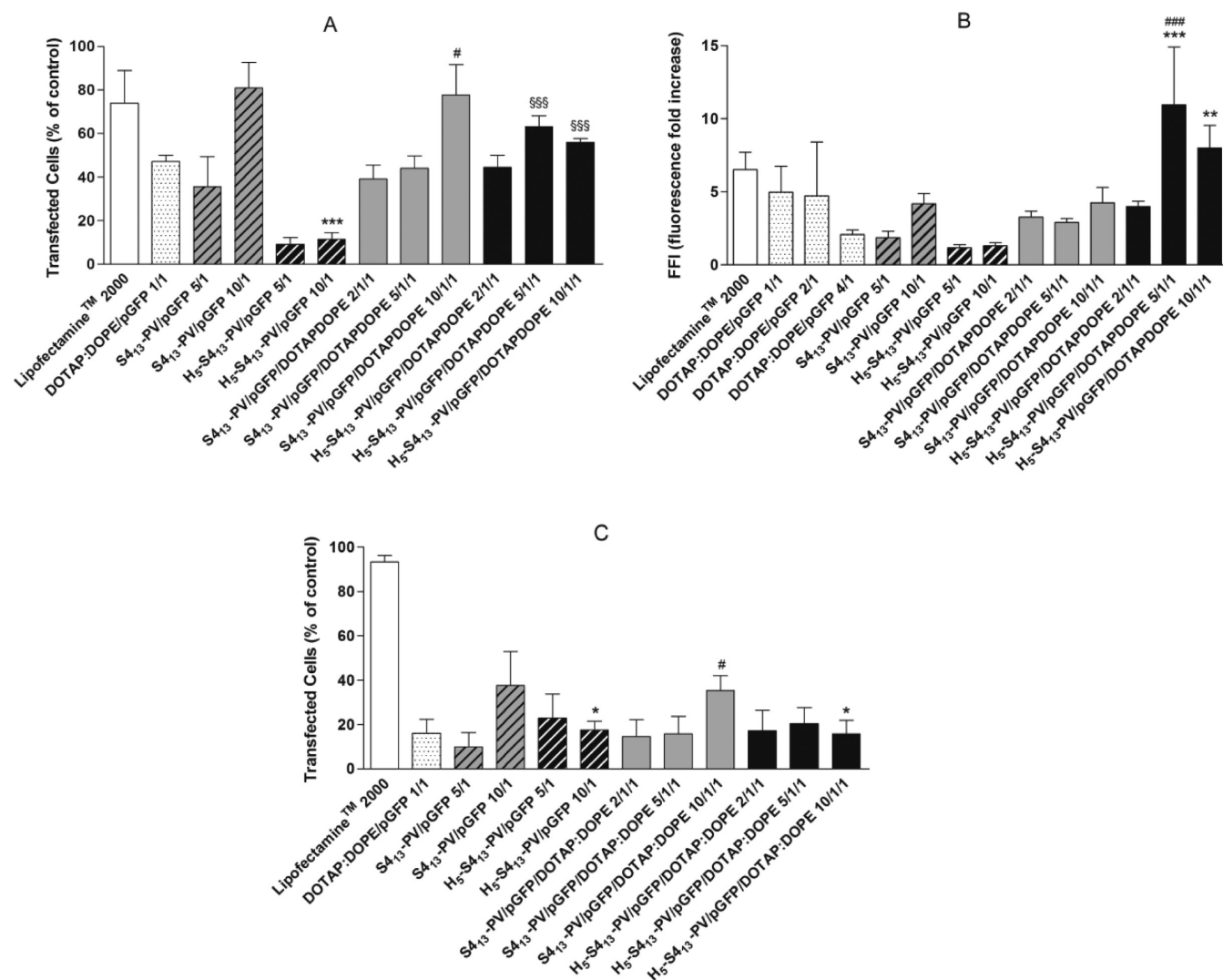
**Figure 2.** Transfection efficiency mediated by different CPP-based systems in HeLa (A and B) and A549 (C) cells. Cells were incubated with the different complexes containing 1 $\mu$g/mL of GFP-encoding plasmid DNA for 4 h at 37 °C, as described in Materials and Methods. Flow cytometry analysis of live cells was performed 48 h after transfection to determine the percentage of transfected cells (A and C) and the increase in cell green fluorescence (B) with respect to the control, nontreated cells, set to 1. Complexes of DNA with DOTAP:DOPE liposomes or Lipofectamine 2000 were used for comparison. All results are presented as the mean $\pm$ SD of at least three independent experiments. Data comparisons were performed between formulations containing S4$_{13}$-PV and H$_5$-S4$_{13}$-PV (*$p < 0.05$; ***$p < 0.001$), between DOTAP:DOPE/pDNA lipoplexes and the same lipoplexes containing S4$_{13}$-PV or H$_5$-S4$_{13}$-PV ($^{\#}p < 0.05$, $^{\#\#}p < 0.01$) and between S4$_{13}$-PV/pDNA or H$_5$-S4$_{13}$-PV/pDNA and the corresponding ternary complexes containing DOTAP:DOPE ($^{\S\S}p < 0.01$; $^{\S\S\S}p < 0.001$).

delivered to each cell, the results indicated that the binary complexes containing the S4$_{13}$-PV or H$_5$-S4$_{13}$-PV peptide delivered a low amount of plasmid copies per cell (Figure 2B). However, ternary complexes containing the H$_5$-S4$_{13}$-PV peptide, prepared at the 5/1/1 and 10/1/1 charge ratios, delivered a higher number of plasmid copies (reflected by a 8–11-fold fluorescence increase relative to the nontreated control cells) than same formulations containing the wild-type CPP (3–4-fold increase relative to the nontreated control cells). These results indicate that the delivery ability of the complexes was increased upon addition of DOTAP:DOPE (2:1 molar ratio) liposomes, this increase being significantly more pronounced in H$_5$-S4$_{13}$-PV/pDNA formulations than in S4$_{13}$-PV/pDNA formulations.

Parallel transfection experiments with ternary complexes composed of either peptide at the 10/1/1 (+/−) charge ratio in the presence of 10% serum were performed. Although the

percentage of transfected cells decreased 11% for complexes formulated with the wild-type peptide, the cell viability was less affected as compared to that observed in the absence of serum (52% cell viability with serum vs 27% without serum). With the histidine-derived peptide-containing complexes, cells maintained a high level of viability, and 33% of cells were successfully transfected (data not shown).

Concerning A549 cells, S4$_{13}$-PV peptide-containing binary and ternary complexes were able to transfect a considerable number of cells, only surpassed by Lipofectamine 2000 (Figure 2C). H$_5$-S4$_{13}$-PV-based plasmid vectors, at the different charge ratios assayed, showed similar or lower transfection efficiencies as compared to those of the corresponding S4$_{13}$-PV/pDNA complexes. For the transfection of these cells, neither S4$_{13}$-PV-nor H$_5$-S4$_{13}$-PV-based formulations benefited from the addition of the lipid component. The fluorescence fold increase relative to the nontreated control cells showed values lower than 1.6 for

all tested conditions, being only significant for the binary complexes composed of the histidine-enriched CPP at the 10/1 charge ratio (data not shown).

**SiRNA Delivery Mediated by S4$_{13}$-PV- and H$_5$-S4$_{13}$-PV-Based Vectors.** In order to select the peptides having the most suitable features to be used in a gene silencing approach, the cytotoxic effects of siRNA delivery systems generated by complexation of the S4$_{13}$-PV peptide or one of its derivatives (H$_5$-S4$_{13}$-PV, reverse NLS, and scrambled) with a siRNA targeting GFP were evaluated in HT1080 GFP-expressing cells (Figure 3).
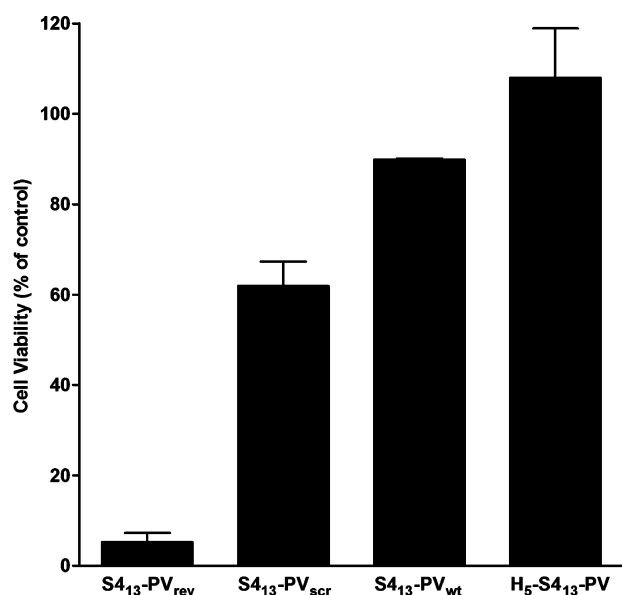


**Figure 3.** Cell viability in the presence of S4$_{13}$-PV, S4$_{13}$-PV$_{scr}$, S4$_{13}$-PV$_{rev}$, and H$_5$-S4$_{13}$-PV peptide-based complexes at a peptide/siRNA charge ratio of 2/1. HT1080 cells were incubated with the different complexes containing 50 nM anti-GFP siRNA, and after 4 h of incubation, the medium was replaced, and the cells were further incubated for 44 h before analysis of cell viability by a modified Alamar Blue assay, as described in Materials and Methods. All results are presented as the mean ± SD of at least three independent experiments.

Significant differences were observed in the cytotoxicity levels induced by binary complexes prepared with the different peptides. The formulations containing S4$_{13}$-PV or its histidine analogue displayed no relevant toxicity (89% and 100% cell viability, respectively). However, cell viability decreased to 61.9% and 5.3% in the presence of complexes containing the scrambled (S4$_{13}$-PV$_{scr}$) and the reverse NLS (S4$_{13}$-PV$_{rev}$) peptides, respectively. Therefore, these complexes were discarded for the experiments of gene silencing, and only the binary complexes that presented low toxicity profiles were evaluated concerning their ability to deliver siRNA (using confocal microscopy) and to induce GFP silencing (using flow cytometry) in HT1080 cells.

Figure 4 displays the internalization pattern of Cy-3-labeled siRNAs delivered to HT1080 cells through complexation with S4$_{13}$-PV or H$_5$-S4$_{13}$-PV, after 4 (Figure 4A−C) or 24 (Figure 4D−F) hours of incubation. Representative flow cytometry histograms (Figure 4G−I) reflecting GFP silencing upon transfection with the same complexes are presented in parallel. Figure 4J summarizes the silencing efficiency of the binary

formulations prepared with each of the four studied peptides, at the 2/1 (+/−) charge ratio, as assessed by flow cytometry.

Confocal studies revealed that siRNA internalization occurred at a similar extent for complexes containing the S4$_{13}$-PV peptide and for those containing Lipofectamine 2000 (data not shown), although a more uniform distribution pattern could be observed when the delivery system included the CPP. However, the superior efficiency of S4$_{13}$-PV binary complexes to mediate siRNA intracellular delivery was not accompanied by an improved GFP knockdown (Figure 4H). In fact, only low levels of biological activity were detected for siRNA/S4$_{13}$-PV complexes. In contrast, the histidine-derivative peptide (H$_5$-S4$_{13}$-PV) was able to promote efficient intracellular siRNA delivery (Figure 4C,F) while simultaneously mediating significant GFP knockdown (Figure 4I). Complexes formulated with this peptide promoted a 69% reduction of GFP levels, while the other peptides did not induce significant silencing or (in the case of S4$_{13}$-PV) induced nonspecific silencing (Figure 4J).

Following the same strategy previously employed to improve S4$_{13}$-PV-mediated pDNA[11] and oligonucleotide[12] delivery, DOTAP:DOPE (1:2 molar ratio) liposomes were added to the formulations containing S4$_{13}$-PV peptide and siRNA, in an attempt to enhance the RNA interference activity of these peptides. Parallel experiments were performed with both the scrambled and reverse NLS peptides in order to determine whether the sequence and structure of this CPP would be involved in the gene silencing activity of the complexes. All possible orders of addition of the components of the ternary complexes were tested, aiming at clarifying the importance of the siRNA "wrapping" by the CPP or by the liposomes to the biological activity of the CPP formulations. Figure 5 (panels A and B) shows typical results obtained for GFP knockdown mediated by the different generated systems. As observed, the differences found in GFP expression when comparing equivalent systems, containing either anti-GFP siRNAs or mut siRNAs, were only significant for DOTAP:DOPE/siRNA and S4$_{13}$-PV-containing systems (Figure 5A and B). It is also possible to note that the protocol of preparation of the ternary complexes did not play a crucial role in gene silencing efficiency. In fact, the addition of cationic liposomes to preformed CPP/siRNA complexes (Figure 5A) and the addition of siRNAs to a mixture of cationic liposomes and CPPs (Figure 5B) resulted in the formation of systems with similar efficiencies, with the latter strategy being only slightly superior. Although a third protocol involving the addition of CPPs to preformed complexes of cationic liposome/siRNA was found to be less efficient (data not shown), the resulting ternary complexes still exhibited considerable biological activity.

When comparing the various CPP-based systems, generated by the addition of siRNAs to a mixture of cationic liposomes and the peptide (Figure 5B), the formulation containing the S4$_{13}$-PV peptide was found to be the most efficient in mediating GFP knockdown. Remarkably, this system was not only significantly more efficient than DOTAP:DOPE/siRNA complexes but also greatly superior to equivalent systems prepared with the reverse NLS, scrambled, or H$_5$-S4$_{13}$-PV peptides. It should be noted that no significant GFP knockdown was observed for H$_5$-S4$_{13}$-PV ternary complexes containing mut siRNAs.

**Survivin Silencing in Different Human Cancer Cell Lines Mediated by S4$_{13}$-PV- and H$_5$-S4$_{13}$-PV-Based Vectors.** Following the demonstration of the feasibility of
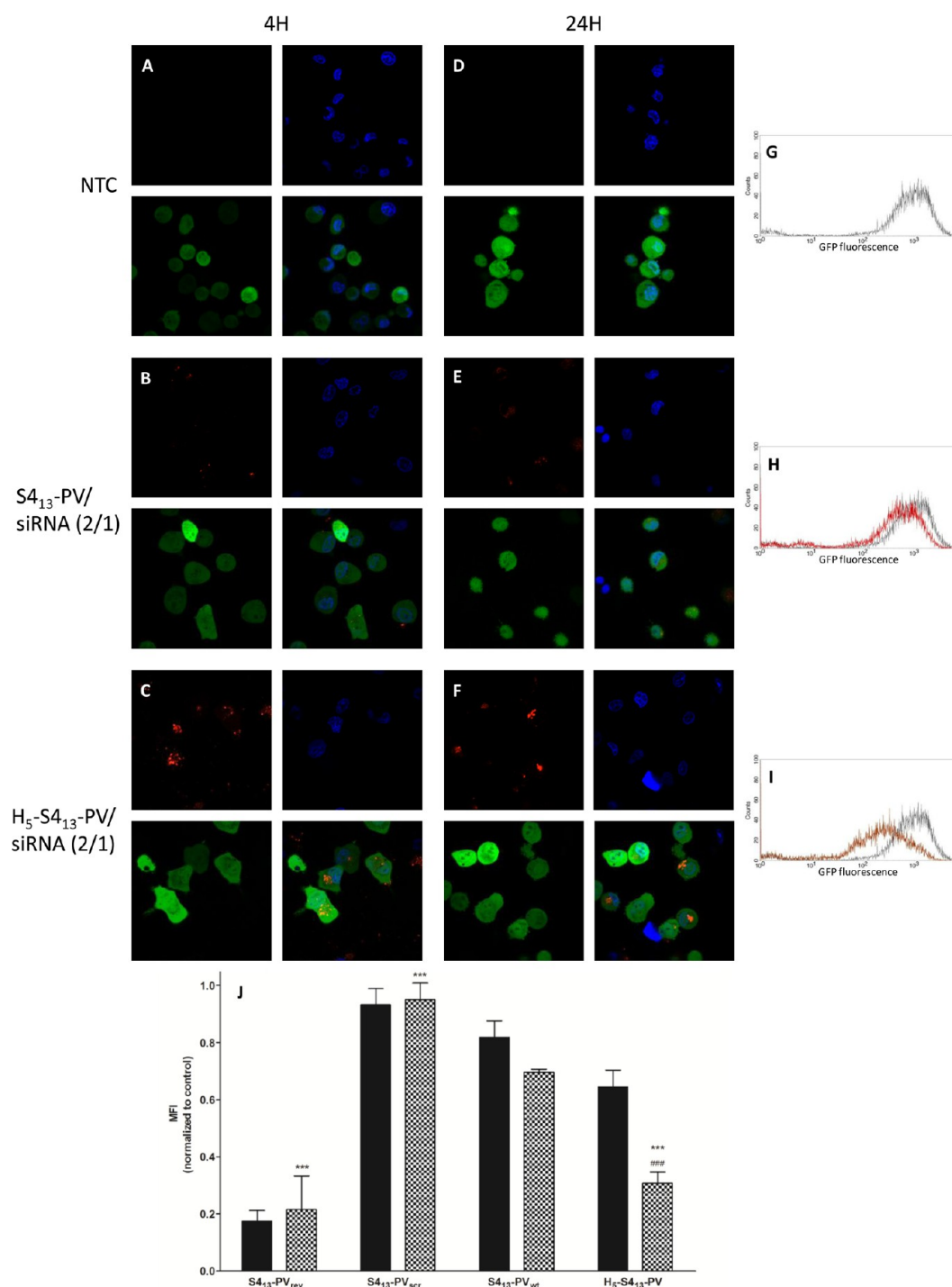
**Figure 4.** SiRNA internalization (A−F) and gene silencing efficiency (G−J) evaluated *in vitro* with different CPP-based systems. For cellular internalization experiments, HT1080 cells (green) were incubated with $S4_{13}$-PV- or $H_5$-$S4_{13}$-PV-based complexes containing 50 nM of mut Cy3-labeled siRNA (red) at the 3/2 charge ratio. Cell nuclei were labeled with Hoechst 33342 dye (blue). Representative confocal microscopy images of each experimental condition (630×), taken upon 4 (A−C) and 24 h (D−F) of cell incubation, are presented. Representative histograms of GFP knockdown obtained by flow cytometry for the same formulations at 48 h post-transfection are also presented (G−I). Results for nontransfected cells (NTC) are shown as a control. GFP knockdown mediated by $S4_{13}$-PV, $S4_{13}$-PV$_{scr}$, $S4_{13}$-PV$_{rev}$, or $H_5$-$S4_{13}$-PV peptide-based complexes at a peptide/siRNA charge ratio of 3/2 was quantified (J). HT1080 cells were incubated with the different complexes containing 50 nM of mut siRNA (■) or anti-GFP siRNA (gray bar). After 4 h of incubation, the medium was replaced, and the cells were further incubated for 44 h before flow cytometry analysis. Data presented in panel J are the mean ± SD of at least three independent experiments. Pairwise comparisons were performed between formulations containing the anti-GFP siRNA and those containing the mut siRNA ($^{###}p < 0.001$) and between $S4_{13}$-PVscr, $S4_{13}$-PVrev, or $H_5$-$S4_{13}$-PV formulations containing the anti-GFP siRNA and the $S4_{13}$-PV formulation containing the same siRNA ($^{***}p < 0.001$). Results for nontreated cells (NTC) were used as a control.

CPP-based delivery systems to mediate GFP knockdown in HT1080 cells, the next step consisted of employing the developed $S4_{13}$-PV and $H_5$-$S4_{13}$-PV delivery systems to silence the endogenous gene survivin using different human tumor cell
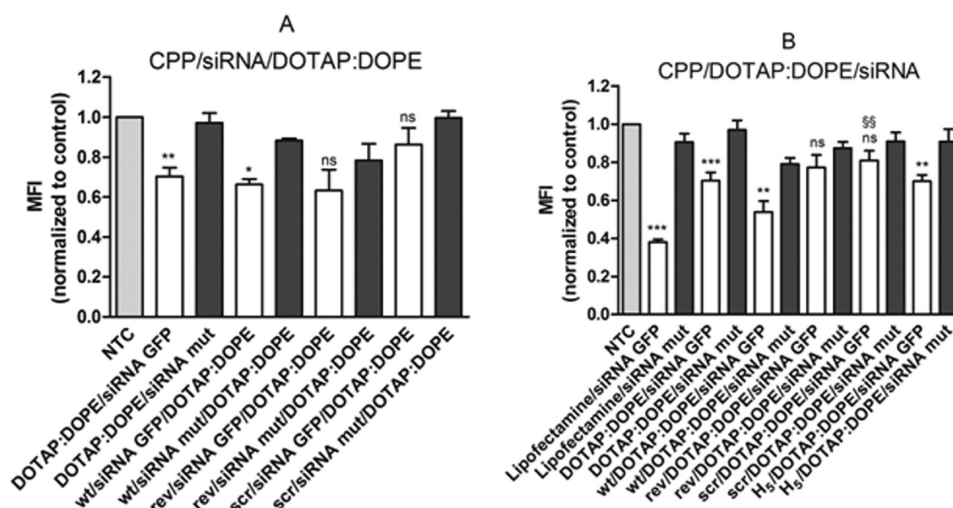
**Figure 5.** GFP knockdown mediated by siRNA complexes prepared with $S4_{13}$-PV (wt), $S4_{13}$-PV$_{scr}$ (scr), $S4_{13}$-PV$_{rev}$ (rev), or $H_5$-$S4_{13}$-PV ($H_5$) and DOTAP:DOPE liposomes at the peptide/lipid/siRNA 4/1/1.5 charge ratio, using two different protocols: addition of cationic liposomes to the preformed CPP/siRNA complexes (A) or addition of siRNAs to a mixture of cationic liposomes and CPPs (B). HT1080 cells were incubated with the different complexes containing 50 nM anti-GFP siRNA for 4 h at 37 °C. Parallel experiments were performed using mut siRNAs. Forty-eight hours post-transfection, the efficiency of GFP knockdown mediated by the different complexes was evaluated by flow cytometry analysis of GFP expression. All results are presented as the mean ± SD of at least three independent experiments. Pairwise comparisons were performed between formulations containing the anti-GFP siRNA and the mut siRNA (*$p < 0.05$, **$p < 0.01$, and ***$p < 0.001$), between the DOTAP:DOPE/anti-GFP siRNA formulation and equivalent formulations containing $S4_{13}$-PV, $S4_{13}$-PV$_{scr}$, $S4_{13}$-PV$_{rev}$, or $H_5$-$S4_{13}$-PV ($^{##}p < 0.01$) and between the lipofectamine/anti-GFP siRNA formulation and equivalent formulations containing $S4_{13}$-PV, $S4_{13}$-PV$_{scr}$, $S4_{13}$-PV$_{rev}$, or $H_5$-$S4_{13}$-PV ($^{§§}p < 0.01$). Results for nontreated cells (NTC) are shown as a control.
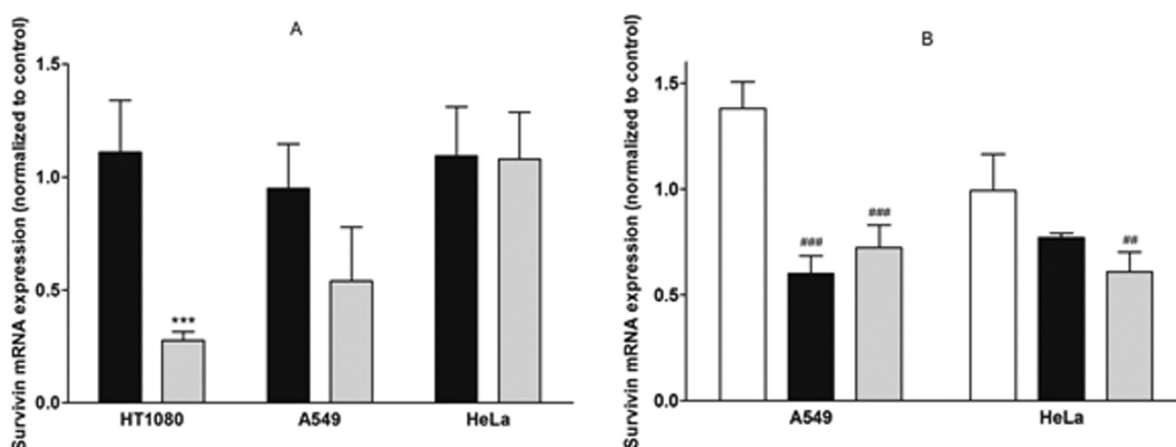


**Figure 6.** Survivin mRNA knockdown mediated by $S4_{13}$-PV and $H_5$-$S4_{13}$-PV peptide-based complexes in HT1080, A549, and HeLa cells. (A) Binary complexes of $S4_{13}$-PV/siRNA (■) or $H_5$-$S4_{13}$-PV/siRNA (gray bar); (B) lipoplexes of DOTAP:DOPE/siRNA (□) and ternary complexes of $S4_{13}$-PV/DOTAP:DOPE/siRNA (■) or $H_5$-$S4_{13}$-PV/DOTAP:DOPE/siRNA (gray bar). Cells were incubated with the different complexes containing 50 nM antisurvivin siRNA for 4 h at 37 °C. Parallel experiments were performed using mut siRNAs. Forty-eight hours post-transfection, the efficiency of survivin knockdown mediated by the different complexes was evaluated by quantitative PCR. For the determination of survivin mRNA levels, RNA was recovered from cells 48 h post-transfection and converted to cDNA, which was analyzed by quantitative PCR. Survivin mRNA expression, determined by the Pfaffl method, as described in the Materials and Methods section, is presented as the changes in RNA transcription caused by the treatment with antisurvivin siRNAs, normalized to RNA transcription changes in cells treated with mut siRNAs (set to 1). All results are presented as the mean ± SD of at least three independent experiments. Data comparisons were performed for each cell line between the formulations containing $S4_{13}$-PV and $H_5$-$S4_{13}$-PV (***$p < 0.001$) and between DOTAP:DOPE/siRNA lipoplexes and the same lipoplexes containing $S4_{13}$-PV or $H_5$-$S4_{13}$-PV ($^{##}p < 0.01$; $^{###}p < 0.001$).

lines toward their potential application in a target gene therapy to cancer. In this context, survivin mRNA and protein levels were determined by QRT-PCR and Western blot, respectively, following the delivery of antisurvivin siRNAs by binary and ternary complexes containing $S4_{13}$-PV or $H_5$-$S4_{13}$-PV.

Figure 6 presents survivin mRNA levels 48 h upon cell transfection with binary complexes, composed of peptide and siRNA (Figure 6A), or with ternary complexes generated by the

addition of siRNA to a mixture of peptide and DOTAP:DOPE liposomes (Figure 6B). The binary delivery systems achieved variable silencing efficiencies, depending on the cell line and on the peptide incorporated in the formulation. While formulations containing the $S4_{13}$-PV peptide were unable to efficiently decrease survivin mRNA levels in the three cell lines tested (HT1080, A549, and HeLa; Figure 6A), complexes containing the $H_5$-$S4_{13}$-PV peptide presented different mRNA knockdown
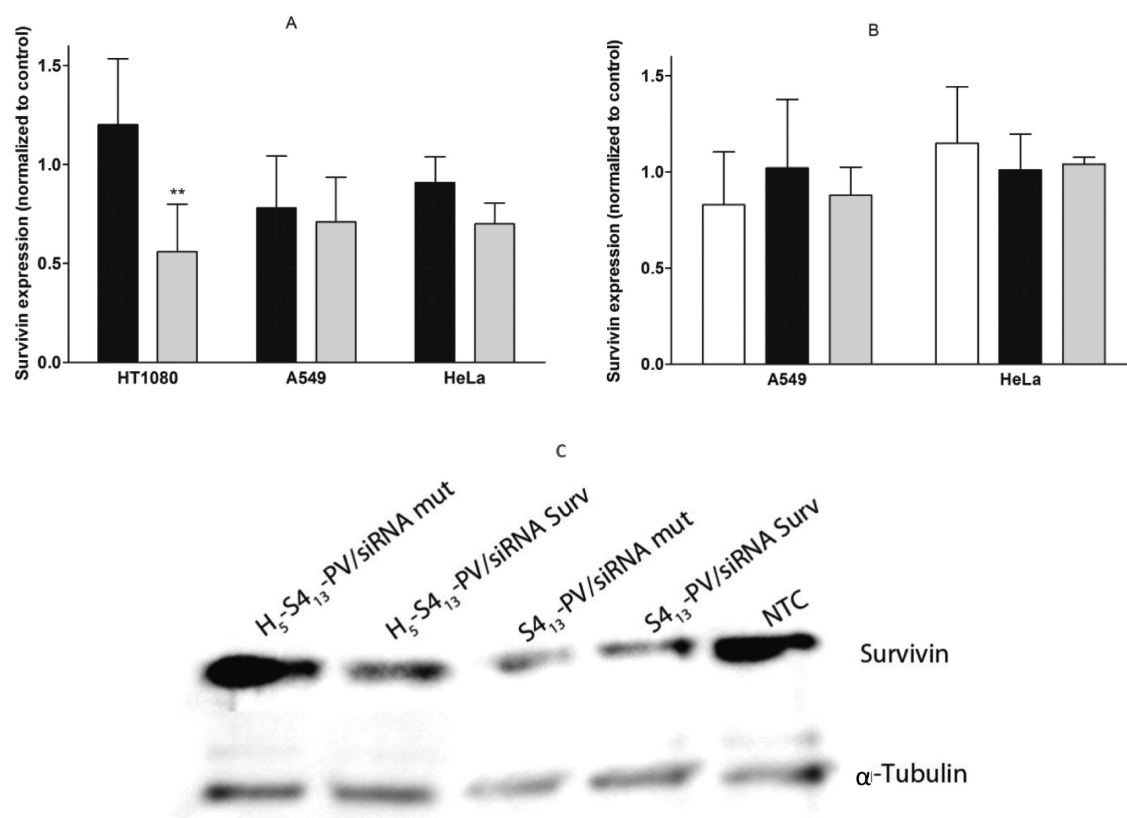
**Figure 7.** Survivin knockdown mediated by S4$_{13}$-PV and H$_5$-S4$_{13}$-PV peptide-based complexes in HT1080, A549, and HeLa cells. (A) Binary complexes of S4$_{13}$-PV/siRNA (■) or H$_5$-S4$_{13}$-PV/siRNA (gray bar); (B) lipoplexes of DOTAP:DOPE/siRNA (□) and ternary complexes of S4$_{13}$-PV/DOTAP:DOPE/siRNA (■) or H$_5$-S4$_{13}$-PV/DOTAP:DOPE/siRNA (gray bar); (C) representative Western blot images illustrating the survivin protein levels in nontreated HT1080 cells (NTC) or following siRNA (targeting survivin or siRNA mut) delivery by S4$_{13}$-PV or H$_5$-S4$_{13}$-PV. Cells were incubated for 4 h at 37 °C, with the different complexes containing 50 nM antisurvivin siRNA. The medium was then replaced, and the cells were further incubated for 72 h before survivin and $\alpha$-tubulin analysis. For each membrane, the analysis of band intensity was performed using Image J software (Wayne Rasband National Institutes of Health, USA). Results in A and B are expressed as survivin fold change with respect to a control (cells treated with the same formulation containing siRNA mut, which was set to 1). Data comparisons were performed for each cell line between formulations containing S4$_{13}$-PV and H$_5$-S4$_{13}$-PV (**$p < 0.01$). All results are presented as the mean $\pm$ SD of at least three independent experiments.

values, varying from 0% silencing in HeLa cells to 50% in A549 cells and 70% in HT1080 cells (Figure 6A). In an attempt to improve survivin silencing in A549 and HeLa cells, DOTAP:DOPE liposomes (1:2 molar ratio) were added to each CPP formulation by complexing the cationic liposomes with the CPP prior to the addition of the siRNA. This strategy was not tested in HT1080 cells based on the results from the experiments on GFP silencing, where its application did not result in any significant improvement (data not shown). Figure 6B shows that the ternary complexes containing the wild-type or the histidine-derivative CPP decreased survivin mRNA levels in the A549 cell line, resulting in 40% and 28% knockdown, respectively. Application of this approach also led to promising results in HeLa cells since 23% and 39% survivin mRNA knockdown were observed for the wild-type and histidine-enriched peptide-containing formulations, respectively. In both cell lines, the silencing effect obtained with lipoplexes containing exclusively the DOTAP:DOPE lipids and siRNA, but no CPP, was negligible. In A549 cells, this formulation appears even to mediate enhanced survivin expression. Therefore, our results, showing a survivin knockdown of 23 to 40% in both cell lines with the ternary systems (S4$_{13}$-PV/DOTAP:DOPE/siRNA and H$_5$-S4$_{13}$-PV/DOTAP:DOPE/siRNA), significantly superior to that obtained with DOTAP:DOPE/siRNA complexes, suggest a clear advantage of

combining the S4$_{13}$-PV peptide or its histidine derivative with the liposome formulation toward the generation of an efficient nonviral siRNA-based antitumoral approach.

Figure 7 presents survivin protein levels, assessed by Western blot analysis and normalized with $\alpha$-tubulin levels, following transfection with both binary and ternary complexes. A pattern similar to that observed for mRNA expression was apparent with binary complexes (Figure 7A). As observed, a superior knockdown of survivin was achieved with complexes containing the histidine-derivative peptide, although the results were only statistically significant for HT1080 cells, in which survivin protein levels decreased 44% (Figure 7A and C). Off-target effects could be observed for binary complexes containing the S4$_{13}$-PV since unspecific silencing was detected following transfection with the mut siRNA, as displayed in Figure 7C. Figure 7B shows survivin protein levels upon cell transfection with ternary complexes containing the DOTAP:DOPE lipids in addition to the CPP (S4$_{13}$-PV or H$_5$-S4$_{13}$-PV) and siRNAs, prepared as previously mentioned. No decrease in the protein expression was achieved with these formulations or with the lipoplexes without CPP, although a decrease in survivin mRNA levels has been observed for the ternary complexes in both A549 and HeLa cells (Figure 6B).

# ■ DISCUSSION

Since the 1970s, when gene therapy was first described,[36] great efforts have been expended toward the discovery of appropriate delivery systems able to surpass the cell membrane and release the different types of nucleic acid molecules, ranging from long DNA molecules to small double-stranded siRNAs, into the target intracellular compartment. Despite the recent advances concerning plasmid DNA and siRNA delivery to target cells, further work should be developed to achieve high levels of cellular uptake and long-term stability, while avoiding unspecific effects, so that nucleic acid therapeutics can reach their full potential as a clinically relevant option.[37−40]

One of the major obstacles for a successful gene therapy strategy results from the impermeability of the cellular membranes to most charged molecules, which has, however, been surpassed by the use of vectors, including cell-penetrating peptides. CPPs constitute a relatively new branch of nonviral vectors that emerged following the description of the RNA/DNA-binding domains of the human immunodeficiency virus (HIV-1) Tat protein[41] and of the *Drosophila* Antennapedia homeodomain protein.[42] Since then, several CPPs have been described and used as delivery systems for nucleic acids and other biomolecules.[4] In the present study, an increase of the length of the $S4_{13}$-PV peptide in five histidine residues was performed taking into account previous observations with the Tat peptide modified with histidine sequences of 5, 10, or 20 residues.[6] On the basis of the fact that the $S4_{13}$-PV is a lysine-rich peptide, lysine residues being mainly concentrated in the NLS at the *C*-terminus of the peptide, the addition of five histidine residues to the other end of the peptide would result in a peptide close to the Tat peptide described by Lo et al.[6] as the most efficient (5His-Tat-5His) regarding the length and positive charge distribution. The additional positive residues have the capacity to facilitate endosomal release but may also favor the establishment of electrostatic interactions between the complexes and the cellular membrane, while potentially increasing nucleic acid protection. The presence of the NLS sequence, although free of histidine residues, added another important function to the new peptide, which is to target pDNA to the nucleus, thereby promoting its transcription.

The transfection efficiency and cell viability levels achieved following pDNA delivery by $S4_{13}$-PV or $H_5$-$S4_{13}$-PV complexes diverged between the two tested cell lines. HeLa cells proved to be more efficiently transfected than A549, although they are also more severely affected in terms of the cytotoxicity exerted by the complexes. In fact, the ability to transfect a high number of cells is often associated with high cytotoxicity. This was also observed with $S4_{13}$-PV-based binary and ternary complexes that transfected the largest number of HeLa cells at charge ratios at which they exerted the highest cytotoxicity, consistent with our previous results.[11] However, the same complexes produced from the histidine-derivative peptide induced low levels of toxicity in both cell types, even at high peptide concentrations (Figure 1). Noteworthy, the $H_5$-$S4_{13}$-PV ternary complexes promoted an elevated percentage of transfected cells and levels of transgene expression higher than those of corresponding complexes with $S4_{13}$-PV (Figure 2B). This effect is most likely linked to the endosomal escape process. The acidification of the endosomal lumen will allow the protonation of the imidazole group in the histidine residues, leading to osmotic swelling and membrane destabilization.[6,7] Moreover, it is possible that, under the acidic conditions in the endosome, the peptide undergoes conformational changes, which may enhance the interaction of the complexes with the endosomal membrane and consequent cytoplasmic release of DNA. This process might have an important outcome in the free nucleic acid yield, directly contributing to the amount of DNA that reaches the cell nucleus. Studies on leucine- and alanine-rich peptides, modified with histidine residues, showed that a histidine-dependent, pH-driven transmembrane-to-in-plane peptide orientation is correlated with high transfection efficiencies,[9] suggesting that pH-dependent membrane insertion of the peptides constitutes an important part of the DNA delivery mechanism. Furthermore, the mechanism of cytoplasmic DNA release may be mediated by membrane interactions with peptide aggregates. Thus, "peptide micelles" may carry away a few lipid molecules from the membranes generating transient openings. Alternatively, peptide monomers or small oligomers can insert efficiently into the membrane, leading to pore formation.[43]

However, the high levels of transgene expression observed for $H_5$-$S4_{13}$-PV ternary complexes as compared to those of the same complexes with $S4_{13}$-PV may be explained by an enhanced uptake of the former. In this regard, complex physicochemical properties, such as size and surface charge, could be on the basis of different cellular uptake yields through the preferential use of distinct internalization pathways. However, in contrast with previous observations,[11,44] physicochemical characterization of the binary and ternary systems revealed no significant differences in terms of size or charge density between complexes with different transfection efficiencies in HeLa cells. In fact, $S4_{-13}PV/pDNA$ complexes at the 5/1 (+/−) charge ratio (1412.0 nm and +9.6 mV) mediated efficient transfection as opposed to $H_5$-$S4_{-13}PV$/pDNA complexes at the same charge ratio, which showed similar size and zeta potential (1108.5 nm and +9.6 mV). However, the lower levels of transfection in A549 cells relative to HeLa cells suggest that these cell lines have different patterns of interaction with the complexes, probably due to the different proteoglycan content at the cell surface or to the preferential use of different internalization pathways that may or may not converge in the endolysosomal route.

The potential of complexes based on $S4_{13}$-PV peptide and its derivatives to promote siRNA delivery was also addressed in HT1080 GFP-expressing cells. In this regard, we aimed at establishing the most suitable peptide structural features, which warrant efficient siRNA-mediated gene knockdown without causing cytotoxicity. Cell viability (Figure 3) indicates that the peptide primary structure plays a crucial role in terms of the cytotoxicity displayed by the corresponding peptide-based complexes. Thus, the reverse NLS peptide, whose amino acid sequence only differs from that of the original peptide in the relative position of three amino acids of the NLS sequence, produces much more toxic complexes compared to the scrambled peptide, which preserves all the $S4_{13}$-PV amino acid residues, although exhibiting a random order. However, as can be observed in Table 1, the proline residue position in the scrambled peptide is maintained with respect to the wild-type and to the histidine-derivative peptides. Proline residues have been suggested to play a relevant role in membrane protein structure and dynamics.[45,46] Proline presents its side chain bonded to the tertiary nitrogen in a cyclic pyrrolidine ring, which makes it the only mammalian imino acid. The consequent absence of a proton in this residue impairs its participation in the formation of hydrogen bonds. This feature

fixes the peptide backbone around proline residues, providing a kink or hinge that constrains the conformation of the adjacent residues[47] and leaves the neighboring carbonyl groups free to participate in alternative hydrogen bonds.[48] Therefore, peptide–siRNA association and interaction of the resulting complexes with the cellular membrane may be affected by the different peptide conformations, which, in the case of the reverse NLS peptide, could be caused by the change of location of the proline residue, leading to a more cytotoxic effect.

The GFP knockdown experiments also shed light on the mechanism of cytotoxicity associated with the use of complexes containing the reverse NLS peptide; the off-target effects of these complexes, reflected on the high silencing activity obtained with the mut siRNA (79%), suggest that theses complexes can strongly interfere with the cellular mechanisms involved in protein synthesis, impairing the production of proteins essential for normal cell function and thus resulting in high toxicity.

The cell internalization extent of siRNA delivered by $S4_{13}$-PV and $H_5$-$S4_{13}$-PV peptide-based complexes, observed by confocal microscopy, correlates with their silencing efficiencies (Figure 4). Consistently, the amount of siRNAs inside the cells transfected with complexes of the wild-type peptide appears to be lower than that inside the cells transfected with histidine-derivative complexes. This observation might be explained by a putatively higher affinity of complexes containing the $H_5$-$S4_{13}$-PV toward the cell surface proteoglycans.

In agreement with what has been previously observed for oligonucleotides,[12] $S4_{13}$-PV peptide/siRNA complexes did not mediate significant gene silencing (Figure 4J). Also consistent with previous studies for plasmid DNA and oligonucleotides, ternary systems combining siRNAs with cationic liposomes and cell-penetrating peptides displayed higher biological activity than binary peptide/siRNA complexes,[9,10] except for the complexes containing the $H_5$-$S4_{13}$-PV peptide (Figures 4J and 5B).

The results presented in Figure 5 show that the protocol of preparation of the ternary complexes, specifically the order of component addition, did not play a crucial role in their gene silencing efficacy, although a small improvement in complex efficiency could be obtained when combining cationic liposomes with the cell-penetrating peptide prior to siRNA addition. Most importantly, the systems containing the $S4_{13}$-PV peptide showed superior biological activity with respect to similar formulations including the reverse NLS or scrambled peptides. This indicates that the amino acid sequence in the $S4_{13}$-PV peptide is required to provide complexes with capacity to promote siRNA internalization and silencing of the target mRNA. The different efficiencies in GFP silencing displayed by the systems containing the $S4_{13}$-PV and reverse NLS peptides corroborate the previous assumption that the location of the proline residue in the NLS sequence should be important for the biological activity of the $S4_{13}$-PV-based complexes. In fact, the NLS sequence per se would not be required for siRNAs to accomplish their function since these molecules do not need to reach the cell nucleus for silencing their target genes.

Since the relevance of a delivery system for potential clinical application can only be fully evaluated in a therapeutic context, we investigated the efficiency of the developed CPP-based systems to mediate silencing of an endogenous gene encoding an oncogenic protein (survivin). This protein presents a huge potential as a therapeutic target in cancer therapy due to its contribution to cancer survival, metastization, and cell

resistance to chemotherapy and radiotherapy.[49] The binary systems containing $S4_{13}$-PV were unable to decrease the mRNA or protein levels of survivin in any of the three cell lines tested (HT1080, A549, and HeLa). In contrast, similar complexes generated from the $H_5$-$S4_{13}$-PV peptide silenced the survivin gene to different extents, depending on the cell line. The highest knockdown effect was obtained in HT1080 cells (73% decrease in mRNA and 44% decrease in protein levels). As would be expected, the ability of the binary $H_5$-$S4_{13}$-PV-based complexes to silence the expression of survivin in HT1080 cells was not statistically different from that observed for GFP (data not shown). The different abilities of the $H_5$-$S4_{13}$-PV peptide-based complexes to silence the survivin gene in different cell lines may be explained by specific features of cells, including internalization preferred pathways, surface proteoglycans content, and metabolic activity. In addition, the different levels of survivin mRNA and protein expression among various tumor cells[50] may contribute to different silencing efficiencies. Importantly, it was shown that the addition of DOTAP:DOPE liposomes, both to $S4_{13}$-PV- and $H_5$-$S4_{13}$-PV-containing systems, led to an increase in mRNA silencing efficiency (Figure 6B). Although the ability of ternary complexes to silence survivin mRNA in both A549 and HeLa cells was superior to that of DOTAP:DOPE/siRNA complexes, the levels of protein knockdown did not follow the same pattern, remaining similar to those observed in cells transfected with lipoplexes devoid of CPP (Figure 7B). This may be due to specific cellular mechanisms that regulate survivin levels in cancer cells. In this regard, some studies have reported the existence of an additional pool of survivin in mitochondria, which can exert its action whenever the levels of cytoplasmic survivin are lower than a defined threshold needed for cancer cell survival.[17,19,51]

Nevertheless, a challenging finding in the present work was that siRNA complexes containing the histidine-enriched $S4_{13}$-PV peptide showed high competence to deliver siRNA into the cells (as demonstrated in GFP-expressing HT1080 cells) and to promote specific knockdown. However, in HeLa cells $H_5$-$S4_{13}$-PV-containing formulations exhibited a transfection efficiency with plasmid DNA comparable to that showed by complexes containing the wild-type peptide, with the advantage of presenting a much lower cytotoxicity.

Overall, our findings reveal that the $H_5$-$S4_{13}$-PV peptide deserves to be further explored aiming at generating efficient nucleic acid delivery-based strategies in the context of therapies for cancer and other diseases. Moreover, our studies on the development of new CPP-based nucleic acid delivery systems and on the establishment of significant structure–activity relationships may open new avenues toward *in vivo* application of increasingly promising gene therapy approaches.

## ■ AUTHOR INFORMATION

### Corresponding Author
*Department of Life Sciences, University of Coimbra, Apartado 3046, 3001-401 Coimbra, Portugal. E-mail: mdelima@ci.uc.pt.

### Present Address
‖S.T.: Stem Cells & Cancer Group, Clinical Research Programme, Spanish National Cancer Research Centre (CNIO), Madrid, Spain.

### Notes
The authors declare no competing financial interest.

## ■ REFERENCES

(1) Fonseca, S. B.; Pereira, M. P.; Kelley, S. O. Recent advances in the use of cell-penetrating peptides for medical and biological applications. *Adv. Drug Delivery Rev.* **2009**, *61*, 953−964.

(2) de Fougerolles, A.; Vornlocher, H.; Maraganore, J.; Lieberman, J. Interfering with disease: a progress report on siRNA-based therapeutics. *Nat. Rev. Drug Discovery* **2007**, *6*, 443−454.

(3) Eguchi, A.; Dowdy, S. F. SiRNA delivery using peptide transduction domains. *Trends Pharmacol. Sci.* **2009**, *30*, 341−345.

(4) Heitz, F.; Morris, M. C.; Divita, G. Twenty years of cell-penetrating peptides: from molecular mechanisms to therapeutics. *Br. J. Pharmacol.* **2009**, *157*, 195−206.

(5) Meade, B. R.; Dowdy, S. F. Enhancing the cellular uptake of siRNA duplexes following noncovalent packaging with protein transduction domain peptides. *Adv. Drug Delivery Rev.* **2008**, *60*, 530−536.

(6) Lo, S. L.; Wang, S. An endosomolytic Tat peptide produced by incorporation of histidine and cysteine residues as a nonviral vector for DNA transfection. *Biomaterials* **2008**, *29*, 2408−2414.

(7) Mason, A. J.; Martinez, A.; Glaubitz, C.; Danos, O.; Kichler, A.; Bechinger, B. The antibiotic and DNA-transfecting peptide LAH4 selectively associates with, and disorders, anionic lipids in mixed membranes. *FASEB J.* **2006**, *20*, 320−322.

(8) Midoux, P.; Monsigny, M. Efficient gene transfer by histidylated polylysine/pDNA complexes. *Bioconjugate Chem.* **1999**, *10*, 406−411.

(9) Kichler, A.; Leborgne, C.; März, J.; Danos, O.; Bechinger, B. Histidine-rich amphipathic peptide antibiotics promote efficient delivery of DNA into mammalian cells. *Proc. Natl. Acad. Sci. U.S.A.* **2003**, *100*, 1564−1568.

(10) Hariton-Gazal, E.; Feder, R.; Mor, A.; Graessmann, A.; Brack-Werner, R.; Jans, D.; Gilon, C.; Loyter, A. Targeting of nonkaryophilic cell-permeable peptides into the nuclei of intact cells by covalently attached nuclear localization signals. *Biochemistry* **2002**, *41*, 9208−9214.

(11) Trabulo, S.; Mano, M.; Faneca, H.; Cardoso, A. L.; Duarte, S.; Henriques, A.; Paiva, A.; Gomes, P.; Simões, S.; Pedroso De Lima, M. C. S4(13)-PV cell penetrating peptide and cationic liposomes act synergistically to mediate intracellular delivery of plasmid DNA. *J. Gene Med.* **2008**, *10*, 1210−1222.

(12) Trabulo, S.; Resina, S.; Simões, S.; Lebleu, B.; Pedroso De Lima, M. C. A non-covalent strategy combining cationic lipids and CPPs to enhance the delivery of splice correcting oligonucleotides. *J. Controlled Release* **2010**, *145*, 149−158.

(13) Ryan, B. M.; O'Donovan, N.; Duffy, M. J. Survivin: a new target for anti-cancer therapy. *Cancer Treat. Rev.* **2009**, *35*, 553−562.

(14) Mesri, M.; Wall, N. R.; Li, J.; Kim, R. W.; Altieri, D. C. Cancer gene therapy using a survivin mutant adenovirus. *J. Clin. Invest.* **2001**, *108*, 981−990.

(15) Tamm, I.; Wang, Y.; Sausville, E.; Scudiero, D. A.; Vigna, N.; Oltersdorf, T.; Reed, J. C. IAP-family protein survivin inhibits caspase activity and apoptosis induced by Fas (CD95), Bax, caspases, and anticancer drugs. *Cancer Res.* **1998**, *58*, 5315−5320.

(16) Li, F.; Ambrosini, G.; Chu, E. Y.; Plescia, J.; Tognin, S.; Marchisio, P. C.; Altieri, D. C. Control of apoptosis and mitotic spindle checkpoint by survivin. *Nature* **1998**, *396*, 580−584.

(17) Hoffman, W. H.; Biade, S.; Zilfou, J. T.; Chen, J.; Murphy, M. Transcriptional repression of the anti-apoptotic survivin gene by wild type p53. *J. Biol. Chem.* **2002**, *277*, 3247−3457.

(18) Beltrami, E.; Plescia, J.; Wilkinson, J. C.; Duckett, C. S.; Altieri, D. C. Acute ablation of survivin uncovers p53-dependent mitotic checkpoint functions and control of mitochondrial apoptosis. *J. Biol. Chem.* **2004**, *279*, 2077−2084.

(19) Dohi, T.; Beltrami, E.; Wall, N. R.; Plescia, J.; Altieri, D. C. Mitochondrial survivin inhibits apoptosis and promotes tumorigenesis. *J. Clin. Invest.* **2004**, *114*, 1117−1127.

(20) Li, F.; Ackermann, E. J.; Bennett, C. F.; Rothermel, A. L.; Plescia, J.; Tognin, S.; Villa, A.; Marchisio, P. C.; Altieri, D. C. Pleiotropic cell-division defects and apoptosis induced by interference with survivin function. *Nat. Cell Biol.* **1999**, *1*, 461−466.

(21) Uchida, H.; Tanaka, T.; Sasaki, K.; Kato, K.; Dehari, H.; Ito, Y.; Kobune, M.; Miyagishi, M.; Taira, K.; Tahara, H.; Hamada, H. Adenovirus-mediated transfer of siRNA against survivin induced apoptosis and attenuated tumor cell growth in vitro and in vivo. *Mol. Ther.* **2004**, *10*, 162−171.

(22) Liu, T.; Biddle, D.; Hanks, A. N.; Brouha, B.; Yan, H.; Lee, R. M.; Leachman, S. A.; Grossman, D. Activation of dual apoptotic pathways in human melanocytes and protection by survivin. *J. Invest. Dermatol.* **2006**, *126*, 2247−2256.

(23) Yonesaka, K.; Tamura, K.; Kurata, T.; Satoh, T.; Ikeda, M.; Fukuoka, M.; Nakagawa, K. Small interfering RNA targeting survivin sensitizes lung cancer cell with mutant p53 to adriamycin. *Int. J. Cancer* **2006**, *118*, 812−820.

(24) Olie, R. A.; Simões-Wüst, A. P.; Baumann, B.; Leech, S. H.; Fabbro, D.; Stahel, R. A.; Zangmeister-Wittke, U. A novel antisense oligonucleotide targeting survivin expression induces apoptosis and sensitizes lung cancer cells to chemotherapy. *Cancer Res.* **2000**, *60*, 2805−2809.

(25) Kappler, M.; Taubert, H.; Bartel, F.; Blümke, K.; Panian, M.; Schmidt, H.; Dunst, J.; Bache, M. Radiosensitization, after a combined treatment of survivin siRNA and irradiation, is correlated with the activation of caspases 3 and 7 in a wt-p53 sarcoma cell line, but not in a mt-p53 sarcoma cell line. *Oncol. Rep.* **2005**, *13*, 167−172.

(26) Collins, J. M.; Leadbeater, N. E. Microwave energy: a versatile tool for the biosciences. *Org. Biomol. Chem.* **2007**, *5*, 1141−1150.

(27) Fields, G. B.; Noble, R. L. Solid phase peptide synthesis utilizing 9-fluorenylmethoxycarbonyl amino acids. *Int. J. Pept. Protein Res.* **1990**, *35*, 161−214.

(28) Carpino, L. A.; Ghassemi, S.; Ionescu, D.; Ismail, M.; Sadat-aalaee, D.; Truran, G. A.; Mansour, E. M. E.; Siwruk, G. A.; Eynon, J. S.; Morgan, B. Rapid, Continuous solution-phase peptide synthesis: application to peptides of pharmaceutical interest. *Org. Process Res. Dev.* **2003**, *7*, 28−37.

(29) Bartlett, G. R. Phosphorus assay in column chromatrography. *J. Biol. Chem.* **1958**, *234*, 466−468.

(30) Bottcher, C. J. F.; van Gent, C. M.; Pries, C. A rapid and sensitive sub-micro phosphorus determination. *Anal. Chim. Acta* **1961**, *24*, 203−204.

(31) Cardoso, A.; Trabulo, S.; Moreira, J. N.; Duzgunes, N.; Pedroso de Lima, M. C. Targeted lipoplexes for siRNA delivery. *Methods Enzymol.* **2009**, *465*, 267−287.

(32) Cardoso, A. L. C.; Simões, S.; de Almeida, L. P.; Plesnila, N.; Pedroso de Lima, M. C.; Wagner, E.; Culmsee, C. Tf-lipoplexes for neuronal siRNA delivery: a promising system to mediate gene silencing in the CNS. *J. Controlled Release* **2008**, *132*, 113−123.

(33) Cardoso, A. L.; Guedes, J. R.; Pereira de Almeida, L.; Pedroso de Lima, M. C. miR-155 modulates microglia-mediated immune response by down-regulating SOCS-1 and promoting cytokine and nitric oxide production. *Immunology* **2012**, *135*, 73−88.

(34) Simões, S.; Slepushkin, V.; Pires, P.; Gaspar, R.; de Lima, M. P.; Düzgüneş, N. Mechanisms of gene transfer mediated by lipoplexes

associated with targeting ligands or pH-sensitive peptides. *Gene Ther.* **1999**, *6*, 1798−1807.

(35) Trabulo, S.; Cardoso, A. L.; Cardoso, A. M. S.; Düzgüneş, N.; Jurado, A. S.; de Lima, M. C. P. Cell-penetrating peptide-based systems for nucleic acid delivery: a biological and biophysical approach. *Methods Enzymol.* **2012**, *509*, 277−300.

(36) Merril, C. R.; Geier, M. R.; Petricciani, J. C. Bacterial virus gene expression in human cells. *Nature* **1971**, *233*, 398−400.

(37) de Fougerolles, A. R. Delivery vehicles for small interfering RNA in vivo. *Hum. Gene Ther.* **2008**, *19*, 125−132.

(38) Pai, S. I.; Lin, Y.-Y.; Macaes, B.; Meneshian, A.; Hung, C.-F.; Wu, T.-C. Prospects of RNA interference therapy for cancer. *Gene Ther.* **2006**, *13*, 464−77.

(39) Ryther, R. C.; Flynt, A. S.; Phillips, J. A., III; Patton, J. G. SiRNA therapeutics: big potential from small RNAs. *Gene Ther.* **2005**, *12*, 5−11.

(40) Oh, Y.-K.; Park, T. G. SiRNA delivery systems for cancer treatment. *Adv. Drug Delivery Rev.* **2009**, *61*, 850−62.

(41) Frankel, A. D.; Pabo, C. O. Cellular uptake of the tat protein from human immunodeficiency virus. *Cell* **1988**, *55*, 1189−1193.

(42) Joliot, A.; Pernelle, C.; Deagostini-Bazin, H.; Prochiantz, A. Antennapedia homeobox peptide regulates neural morphogenesis. *Proc. Natl. Acad. Sci. U.S.A.* **1991**, *88*, 1864−1868.

(43) Marquette, A.; Mason, A. J.; Bechinger, B. Aggregation and membrane permeabilizing properties of designed histidine-containing cationic linear peptide antibiotics. *J. Pept. Sci.* **2008**, *14*, 488−495.

(44) Cardoso, A. M.; Faneca, H.; Almeida, J. A.; Pais, A. A.; Marques, E. F.; de Lima, M. C. P.; Jurado, A. S. Gemini surfactant dimethylene-1,2-bis(tetradecyldimethylammonium bromide)-based gene vectors: a biophysical approach to transfection efficiency. *Biochim. Biophys. Acta* **2011**, *1808*, 341−351.

(45) Williams, K. A.; Deber, C. M. Proline residues in transmembrane helices: structural or dynamic role? *Biochemistry* **1991**, *30*, 8919−8923.

(46) Cordes, F. S.; Bright, J. N.; Sansom, M. S. P. Proline-induced distortions of transmembrane helices. *J. Mol. Biol.* **2002**, *323*, 951−960.

(47) Carver, E R; Blout, J. P. Polypeptide Models for Collagen. In *Treatise on Collagen*; Ramachandran, G. N., Ed.; Academic Press: London, 1967; pp 441−523.

(48) Veis, A.; Nawrot, C. Basicity differences among peptide bonds. *J. Am. Chem. Soc.* **1970**, *92*, 3910−3914.

(49) Altieri, D. C. New wirings in the survivin networks. *Oncogene* **2008**, *27*, 6276−6284.

(50) Li, F. Survivin study: what is the next wave? *J. Cell. Physiol.* **2003**, *197*, 8−29.

(51) Dohi, T.; Altieri, D. C. Mitochondrial dynamics of survivin and "four dimensional" control of tumor cell apoptosis. *Cell Cycle* **2005**, *4*, 21−23.